A role for FoxN3 in the development of cranial cartilages and muscles in *Xenopus laevis* (Amphibia: Anura: Pipidae) with special emphasis on the novel rostral cartilages

Jennifer Schmidt,[1] Maximilian Schuff[2] and Lennart Olsson[1]

[1]*Institut für Spezielle Zoologie und Evolutionsbiologie mit Phyletischem Museum, Friedrich-Schiller-Universität, Jena, Germany*
[2]*Institut für Biochemie, Universität Ulm, Ulm, Germany*

Abstract

The origin of morphological novelties is a controversial topic in evolutionary developmental biology. The heads of anuran larvae have several unique structures, including the supra- and infrarostral cartilages, the specialised structure of the gill basket (used for filtration), and novel cranial muscle arrangements. FoxN3, a member of the *forkhead/*winged helix family of transcription factors, has been implicated as important for normal craniofacial development in the pipid anuran *Xenopus laevis*. We have investigated the effects of functional knockdown of FoxN3 (using antisense oligonucleotide morpholino) on the development of the larval head skeleton and the associated cranial muscles in *X. laevis.* Our data complement earlier studies and provide a more complete account of the requirement of FoxN3 in chondrocranium development. In addition, we analyse the effects of FoxN3 knockdown on cranial muscle development. We show that FoxN3 knockdown primarily affects the novel skeletal structures unique to anuran larvae, i.e. the rostralia or the fine structure of the gill apparatus. The articulation between the infrarostral and Meckel's cartilage is malformed and the filigreed processes of the gill basket do not develop. Because these features do not develop after FoxN3 knockdown, the head morphology resembles that in the less specialised larvae of salamanders. Furthermore, the development of all cartilages derived from the neural crest is delayed and cranial muscle fibre development incomplete. The cartilage precursors initially condense in their proper position but later differentiate incompletely; several visceral arch muscles start to differentiate at their origin but fail to extend toward their insertion. Our findings indicate that FoxN3 is essential for the development of novel cartilages such as the infrarostral and other cranial tissues derived from the neural crest and, indirectly, also for muscle morphogenesis.

Key words forkhead box genes; muscle morphogenesis; neural crest; novelties; rostralia; *Xenopus laevis*.

Introduction

The morphology of anuran larvae is substantially different from that of other vertebrates owing to the presence of rostralia in the upper and lower jaw skeletons and other specialisations that decouple larval and adult ecologies. The evolutionary success (measured, for example, as species number) of frogs in contrast to other recent amphibians is probably associated with this innovation, which facilitates herbivory in the larvae. This opened up a new feeding niche for frog larvae (scraping algae), and has been suggested to be an important factor behind the evolutionary success of anurans in relation to other groups of recent amphibians (Svensson & Haas, 2005). *Xenopus laevis* has a highly derived tadpole stage with a filigreed structure of the gill basket necessary for filter feeding in addition to the extra mouth structures present as unique novelties in frog tadpoles, which are slightly modified in *X. laevis*. In this species, the infrarostral cartilages, which articulate with Meckel's cartilage in the lower jaw, are fused medially (Sokol, 1977) and the suprarostral cartilage is a crescent-shaped plate that supports the tentacular cartilage in the upper jaw (Trueb & Hanken, 1992). The origin of the rostralia is unresolved (De Sa & Swart, 1999; Svensson & Haas, 2005). Is it the

Correspondence

Jennifer Schmidt, Institut für Spezielle Zoologie und Evolutionsbiologie mit Phyletischem Museum, Friedrich-Schiller-Universität, Erbertstr. 1, 07743 Jena, Germany. T: + 49 3641949165; F: + 49 3641949162; E: jennifer.schmidt@uni-jena.de

cartilages themselves that are novelties, or is it rather the articulation between them that is an evolutionary novelty? If the latter is the case, the infrarostrals are partitioned off from Meckel's cartilage and the suprarostrals from the trabecular horns. Changes in developmental processes and mechanisms must underlie the appearance of novel anatomical structures, but the way these work remains a challenging question.

The cells composing the novel head skeletal structures are derived from the neural crest (NC) (Gross & Hanken, 2008). The neural crest is a transient population of cells that is unique to vertebrates and that gives rise to different types of tissues, including neurones, cranial ganglia, glia and pigment cells, the sclera and cornea of the eye, and skeletal and dental tissues. The cranial development and morphology of different anuran tadpoles and other amphibian larvae have been investigated (reviewed by Hall & Hörstadius, 1988; Hall, 2009), but the molecular mechanisms of incipient chondrogenesis, and the morphogenesis of the NC-derived jaw and skull elements are only partly known in recent amphibians. Based on study of tissue cultures of the neural folds and pharynx endoderm of the Alpine newt (*Triturus alpestris*), Epperlein & Lehmann (1975) defined three stages of the NC-derived chondrocyte lineage: (i) prechondroblasts, (ii) chondroblasts and (iii) chondrocytes. Chondrogenesis induction is mediated by different extrinsic and intrinsic signals (Francis-West et al. 1998; Santagati & Rijli, 2003). In amphibians, NC cells must be in contact with the underlying pharyngeal endoderm to evoke chondrogenesis (Seufert & Hall, 1990). Although the mechanisms and processes of chondrogenesis are known primarily from studies of limb bud development, little is known about the detailed mechanisms of chondrogenesis of the NC-derived chondrocyte lineage (Hall & Miyake, 1992; Hall, 2005).

Neural crest cells also contribute directly to cranial muscle connective tissue in some species (chicken, Noden, 1983a,b; Couly et al. 1992; Fire-bellied toad, Olsson et al. 2001; Mexican axolotl, Ericsson et al. 2004). Vertebrate cranial muscles are derived from cranial paraxial mesoderm that originates from restricted areas ventrolateral to the corresponding rhombomeres (Edgeworth, 1935; Noden, 1983a,b; Couly et al. 1992; Trainor & Tam, 1995; Schilling & Kimmel, 1997). The muscle progenitors maintain a constant permanent nearest-neighbour relation with adjacent, overlying NC cells when populations of both kinds of cells reach the sites of their morphogenesis within the branchial arches; these mesenchymal populations elongate to their final position together (Evans & Noden, 2006). The development of craniofacial structures and muscles requires intricate spatiotemporal signalling interactions among molecules, specialised cell types and tissues (Noden & Trainor, 2005; Noden & Francis-West, 2006). The detailed processes involved in the positional guidance remain unclear. Due to this, principal questions concern (i) the process of cartilage formation from NC cells and (ii) the role of NC cells in the patterning of cranial muscles. Several factors have been implicated in the migration, determination and maintenance of NC cells, including several signalling cascades, e.g. the FGF, BMP and Wnt pathways (Barembaum & Bronner-Fraser, 2005), as well as the Sox family (Sox8, Sox9, Sox10; Hong & Saint-Jeannet, 2005), the Pax family (Pax3; Sato et al. 2005), and several forkhead transcription factors (e.g. FoxD1, FoxD3; Dottori et al. 2001; Gomez-Skarmeta et al. 1999). Recently, FoxN3, another member of the *forkhead box* gene family was shown to be important for craniofacial development in *X. laevis* and in the mouse (Schuff et al. 2007; Samaan et al. 2010). Some of the effects in *X. laevis* of *FoxN3* depletion in head cartilages and cranial nerves were described by Schuff et al. (2007). The present study thoroughly describes the effects on cranial muscle anatomy and development, and also gives a more complete account of the effects of FoxN3 knockdown on the anatomy and development of NC-derived cartilages, with a focus on evolutionarily novel structures, such as the rostralia and the complicated fine structure of the gill basket.

Materials and methods

Xenopus embryo culture and manipulation

Xenopus laevis from the breeding colony at the University of Ulm were used in this study. Harvesting of eggs, fertilisation and embryo culture were done in 0.1× modified Barth's solution (MBSH) at 16 °C. Oocytes were obtained from induced spawning using human choriongonadotropin, raised at 15 °C until the desired stages and staged according to the normal table (Nieuwkoop & Faber, 1994) .

A FoxN3 antisense oligonucleotide (FoxN3-MO) was derived from the first 25 nucleotides of the translation start of the FoxN3 gene (5′-ACTAGGAGGGCATGACTGGACCCAT-3′; Gene Tools, USA) as previously described by Schuff et al. (2007). The FoxN3 morpholino inhibits translation of FoxN3 and binds to all splice variants of FoxN3 (Schuff et al. 2006; Schuff et al. 2007). Morpholino injections were performed in 4% Ficoll∕0.5× MBSH. FoxN3-MO was injected in doses of 15–17 ng into one or two blastomeres of two-cell stage embryos. For control, a standard control morpholino oligonucleotide (Co-MO) against the sequence of the human *β-globin* gene 5′-CCTCTTACCTCAGTT-ACAATTTATA-3′ (Gene Tools) was injected under identical conditions.

Histology

A total of 99 embryos and larvae in Stages 36–46 were fixed in 4% phosphate-buffered formalin (PFA). For each of the stages (36, 37, 38, 39, 40, 42, 44, 46), three, four or five embryos were used in each of the three categories of experiments (control, unilaterally injected, bilaterally injected). Embryos were embedded in paraffin for serial sectioning according to Böck (1989) and sections of 7 μm thickness were cut with a rotary microtome (HM360 Microm, Germany). Paraffin sections were stained according to Heidenhain's Azan technique (Böck, 1989). Thirty Stage-46 larvae were whole-mount stained for cartilage with

Alcian blue using the standard protocol of Taylor & Van Dyke (1985), and a subset also was stained for muscles using a monoclonal antibody against newt skeletal muscle (monoclonal antibody 12∕101; Kintner & Brockes, 1984) and the Ultra Vision detection System (Thermo Scientific, Canada). Images of cross-sections were produced with an Axioplan microscope (Zeiss, Germany) fitted with a ColorView12™ camera (Olympus Soft Imaging System, Germany) using the program Analysis®3.2 (Olympus Soft Imaging System). Images of whole-mount stained larvae were acquired with a Stemi SV11 stereo microscope (Zeiss) with a ColorViewIII™ camera and Analysis®3.2.

X-ray-based micro-computed tomography and computer-based 3D-reconstruction

The X-ray-μCT of uni- and bilaterally FoxN3-MO-injected *X. laevis* tadpoles, as well as of uninjected controls (Stage 46) was performed using the Xradia MicroXCT system at the Department of Theoretical Biology, University of Vienna. The formalin-fixed specimens – four unilaterally injected, four bilaterally injected and two control specimens – were stained with phosphotungstic acid to obtain optimal contrast between different tissues (Metscher, 2009). For tadpoles at this stage of development, no variation in the phenotype produced by uni- or bilateral injection of FoxN3-MO, respectively, could be observed, except for the geniohyoideus muscle. In the entire material investigated at this stage (15 tadpoles), the geniohyoideus muscle was missing in three tadpoles, two bilaterally and one unilaterally injected, and shortened in the other injected specimens. Based on the μCT-image stack of a unilaterally injected tadpole, a 3D reconstruction of the head was performed using Bitplan Imaris 6.1.5 software (Bitplan AG, Switzerland). To create the surface objects, the head muscles and cartilages were outlined manually on every second image. Then data files were transferred to Alias® Maya 7.0 software (Alias Wavefront, Canada) for assembly of the different reconstructed structures. In addition, we used Maya to smooth slightly all structures to minimise artefacts of the surface remodelling; this produced no relevant changes in arrangement or general shape. A movie that first rotates the model of the chondrocranium of a unilaterally injected tadpole, and then adds the cranial musculature and makes another rotation, was made in Maya. The movie can be downloaded as Supporting Information to aid the understanding of the anatomical structures and their malformations.

Results

We used the morpholino technique to examine the effects of uni- and bilateral functional knockdown of FoxN3 on *Xenopus laevis* tadpole head development and anatomy. We focused on malformations of skeletal and muscle tissues, as seen using conventional histology, whole-mount staining of cartilage and muscles, and X-ray micro-computed tomography followed by 3D reconstruction. When we compiled the experimental data, detailed comparisons showed that in FoxN3-depleted larvae, the injected side of unilaterally injected larvae showed the same malformations as occurred on both sides in bilaterally injected specimens. The control side in unilaterally injected larvae had the same normal morphology as seen in control specimens. This has

been noted in earlier studies (Maurus et al. 2005; Schuff et al. 2007; Schuff et al. 2010). Therefore, the following comparison of the affected side in unilaterally injected embryos with the control side also implicitly includes a comparison with uninjected control specimens. FoxN3-depleted tadpoles show no visible differences to the normal phenotype until Stage 39, afterwards oedema in the head and trunk region and significantly stunted growth are observed (Fig. 1A).

Cartilage formation

Following functional knockdown of FoxN3, only NC-derived cartilages are malformed; the basihyal, basibranchial and otic capsule, which are likely to be mainly mesoderm-derived (Gross & Hanken, 2008), are not affected. All cartilages were smaller than those on the control side (Fig. 1B), but the extent to which they were malformed varied between cartilages (see below for details). The craniofacial skeleton is asymmetrical and the injected side flattened, in contrast to the control side (Fig. 2A,B). All NC-derived cartilages are affected and all injected specimens show a delay in chondrocyte differentiation on the injected side. Cartilage precursors initially condense in their proper positions but later differentiate incompletely, leaving free, uncondensed chondroblasts around different structures.

The most anterior elements, derived from the mandibular arch, form the upper and lower jaws. Upon knockdown of FoxN3, they are reduced and deformed (Fig. 2D). The infrarostral cartilage is elongated caudally and bears a malformed articulation with Meckel's cartilage (Fig. 3B). The anlagen of the infrarostral cartilage normally develop rostral to Meckel's cartilage, but in the knockdown specimens they develop on the same level as Meckel's cartilage. Moreover, the cellular anlagen of the infrarostral cartilages are shifted to a more median position and abut the anlagen of Meckel's cartilage laterally (Fig. 4E,F). No articulation forms between the infrarostral and Meckel's cartilage. Meckel's cartilage is elongated rostrally and curves to the rostral margin of the infrarostral cartilage instead of to the lateral margin (Fig. 2D). Moreover, the larval jaw articulation does not form. The palatoquadrate and Meckel's cartilage are arranged in close proximity to each other and fail to establish an articulated joint, the same type of malformation that is seen between the infrarostral and Meckel's cartilages (Fig. 3C). The palatoquadrate and Meckel's cartilage originate from the same mesenchymal cell condensation and normally diverge to make a ventral connection with an interzone, but in these individuals they formed two distinct cartilages that lack an intervening interzone in which the jaw joint could form. The part of the neurocranium derived from the mandibular NC stream is shortened and the development of the commisura quadratocranialis, the rostral connection of the palatoquadrate cartilage to the neurocranium, is delayed (Fig. 4G,H). Additionally, distinct parts of
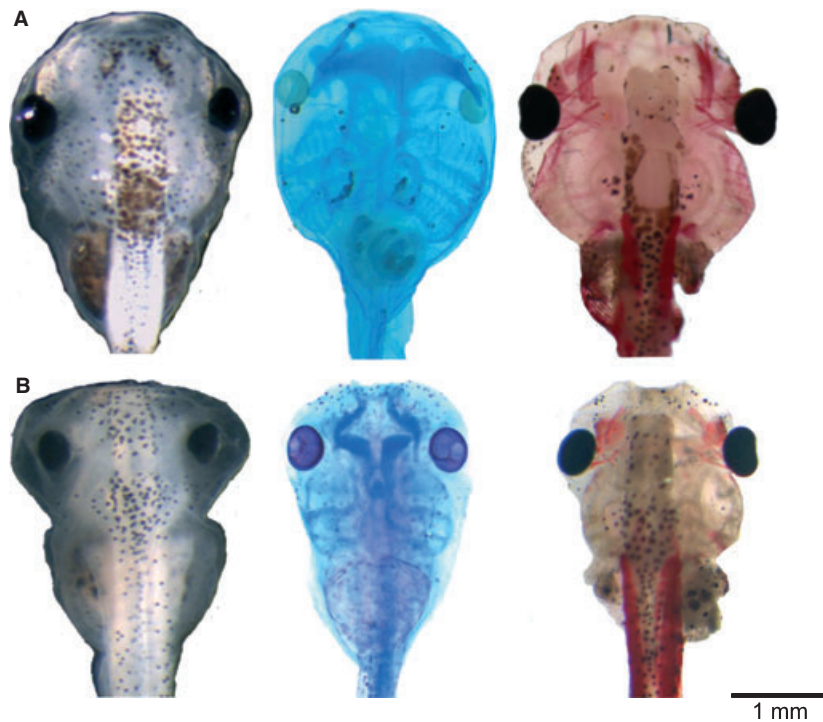
Fig. 1 Effects of FoxN3-MO injections on the cranial external morphology, cartilage anatomy (Alcian-stained cartilage appear dark blue), and muscle morphology (muscle stained with newt skeletal muscle antibody) in *X. laevis* larva at Stage 46. (A) Co-MO-injected tadpole with normally formed skull (left), cartilage (middle), and muscle (right) anatomy. (B) FoxN3-MO (bilaterally)-injected tadpole has a significantly smaller skull with several oedema formations in head and trunk region (left), combined with smaller and malformed cartilage (middle) and muscle (right) results from FoxN3-MO injection. All images are dorsal views of larval skulls with the anterior up.

processes were lost, e.g. the processus ascendens palato-quadrati is shortened or missing (Fig. 2A,B). The anlage of the processus ascendens palatoquadrati forms but does not condense and differentiate into cartilages. Thus, the distal end of the process is missing and no caudal connection to the neurocranium is formed (Fig. 3E). The distal end often is broadened and has a free end.

The ceratohyal cartilage, derived from the hyoid NC stream, is distorted and reduced in size (Fig. 2C). The processus anterior hyalis does not form and both the processus lateralis hyalis and posterior hyalis are short but broad (Fig. 3E). The cell condensation at the anterior end of the anlage is smaller and does not elongate further rostrally (Fig. 4K,L). Additionally, the cellular anlage is larger medially than in the controls and is only partially elongated caudally. In two of the four unilaterally injected tadpoles, both sides of the ceratohyal cartilage are malformed (Fig. 3D). Furthermore, the movable connection between the two cartilages is undeveloped and the cartilages rest against each other in the middle.

The branchial basket, derived from the anterior and posterior branchial NC streams, is asymmetrical and the ceratobranchial cartilages are shortened (Fig. 2D). Given that the ceratobranchial cartilages are flattened, it follows that the gill slits are shifted to the ventral side (Fig. 2C). Cell condensation normally is completed at Stage 45, but in the FoxN3-depleted larvae the last two ceratobranchial cartilages are incompletely condensed. Moreover, the cartilage bridges between the individual ceratobranchial cartilages are incompletely formed (Fig. 3F). The development of the cellular anlage of the branchial basket is delayed and the branchial basket is smaller than that of the control. The underdeveloped branchial basket made it difficult to follow the muscle differentiation of the branchial muscles connected to it. The short cartilaginous processes of the branchial basket also are lost (Fig. 3F). The anlagen of the processes form but do not develop properly, in the same manner in which the ascending process does not complete development.

Musculature

Functional knockdown of FoxN3 produces a wide variety of muscle malformations, with some muscles having incomplete differentiation, shifts of insertion, and anastomoses. The insertions of muscles are often frayed and disordered. Detailed changes and malformations of all muscles are listed in Table 1. We found no malformations in laryngeal muscles. Similarly, we observed no abnormalities in the ocular muscles, save for the final patterning of three ocular
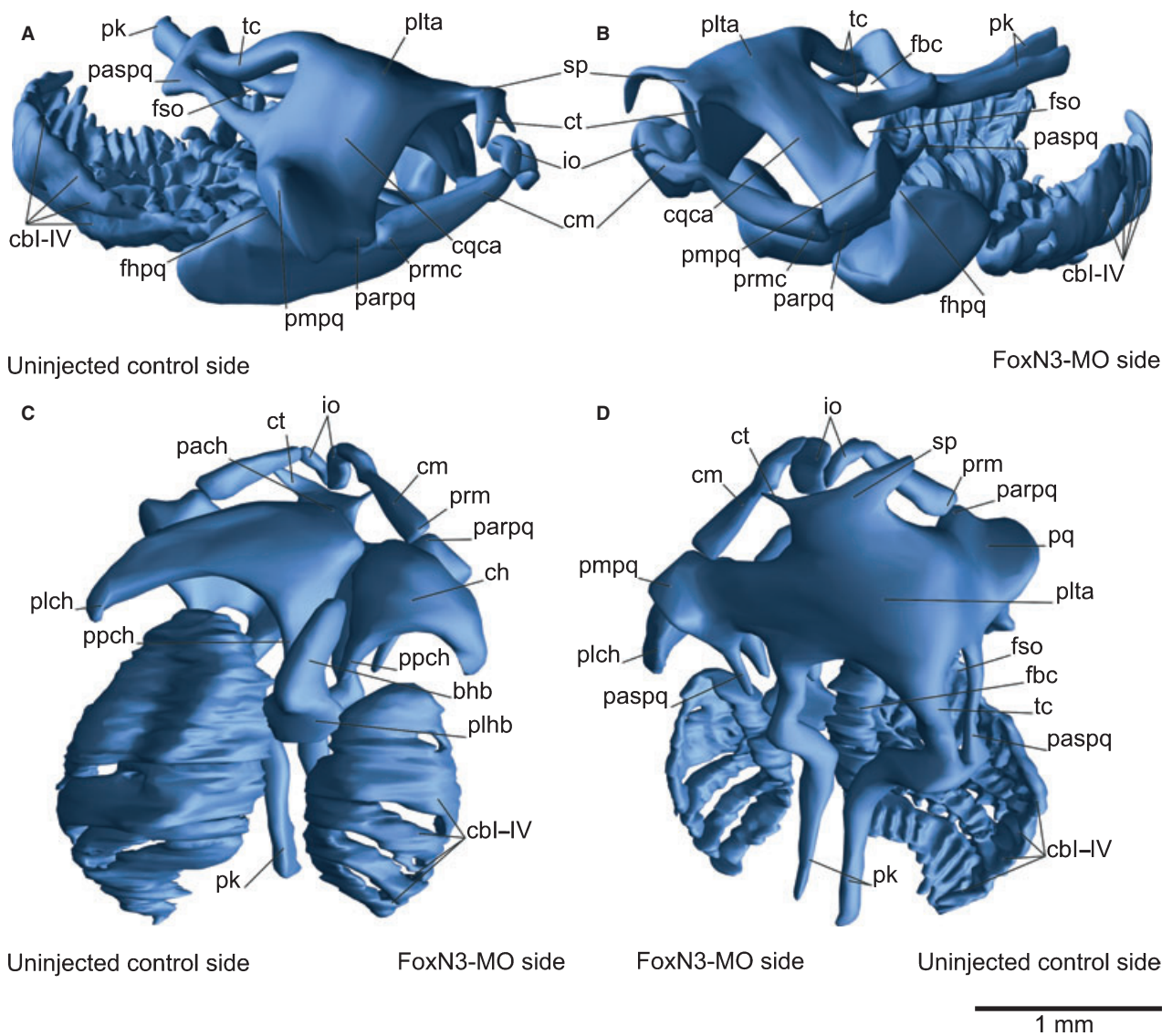
Fig. 2 Three-dimensional reconstruction of the skull of an unilaterally FoxN3-MO-injected *X. laevis* larva at Stage 46 in lateral (A,B), ventral (C) and dorsal (D) views. FoxN3 knockdown primarily affects novel skeletal structures, thus the gill basket is much simplified, due to loss of the filigreed structures, and the rostral cartilages are malformed. Furthermore, all cartilages are smaller, variously malformed and several processes are lost in FoxN3-depleted tadpoles. bhb, basihyobranchial; cbI–IV, ceratobranchials I–IV; ch, ceratohyal; cm, Meckel's cartilage; cqca, commisura quadratocranialis anterior; ct, cornuae trabeculae; fbc, Fenestra basicranialis; fhpq, facies hyoidis of the palatoquadrate; fso, fenstra subocularis; io, infrarostral; pach, processus anterior hyalis; parpq, processus articularis palatoquadrati; paspq, processus ascendens palatoquadrate; pk, parachordals; plch, processus lateralis hyalis; plhb, planum hypobranchiale; plta, planum trabeculare anticum; pmpq, processus muscularis palatoquadrati; ppch, processus posterior hyalis; pq, palatoquadrati; prmc, processus retroarticularis of Meckel's cartilage; sp, suprarostral plate; tc, trabeculae cranii.

muscles. The insertions of the m. rectus posterior and the mm. rectus superior et inferior are shifted dorsally and the origin of the m. rectus superior is fused with that of the mm. rectus inferior et posterior (Fig. 5A,B). In addition, the development of the first myoblasts, which appear about two stages later than in controls, is delayed (Tables 2 and 3). Several visceral arch muscles start to differentiate correctly at their origin but fail to extend toward their insertions and show incomplete development of muscle fibres.

Mandibular arch musculature

The development of the six (paired) mandibular arch muscles is delayed during the first 4 days following functional knockdown of FoxN3 (Fig. 4B,C); these are the levator mandibulae longus group, the levator mandibulae articularis et externus, and the intermandibularis (Sedra & Michael, 1957). Muscles in the mm. levator mandibulae longus group, which share a common origin, extend rostrally in a horizontal rostromedial plane, not
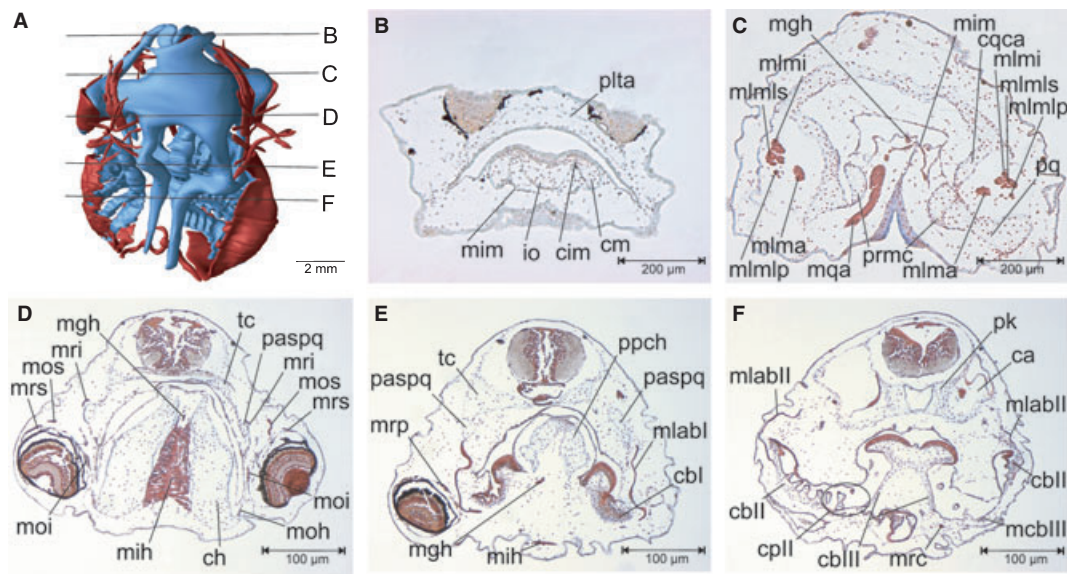
Fig. 3 (A) Three-dimensional reconstruction of the skull and cranial muscles of an unilaterally FoxN3-MO-injected *X. laevis* larva at Stage 46, dorsal view showing the level of the transverse sections B–F. (B–F) Transverse sections of the head. Following FoxN3 knockdown, different malformations of the cranial muscles and cartilages can be seen at the injected side (right) compared to the control side (left), for example loss of the articulation between the infrarostral and Meckel's cartilages and of the jaw articulation (B,C), muscle malformation of mih (D) or shortening of the psapq or loss of the filigreed processes of the gill basket (E,F). cbl–III, ceratobranchials I–III; ch, ceratohyal; cm, Meckel's cartilage; cpll, commisura proximalis II; cqca, commisura quadratocranialis anterior; io, infrarostral; mcbIII, mm. constrictores branchiales III; mgh, m. geniohyoideus; mih, m. interhyoideus; mim, m. intermandibularis; mlab I–II, mm. levator arcuum branchialium I–II; mlma, m. levator mandibulae anterior; mlmi, m. levator mandibulae inferior; mlmlp, m. levator mandibulae longus profundus; mlmls, m. levator mandibulae longus superior; moi, m. obliquus inferior; moh, m. orbitohyoideus; mos, m. obliquus superior; mrc, m. rectus cervicis; mri, m. rectus inferior; mrp, m. rectus posterior; mrs, m. rectus superior; paspq, processus ascendens palatoquadrati; pk, parachordals; plta, planum trabeculare anticum; ppch, processus posterior hyalis; pq, palatoquadrate; prmc, processus retroarticularis of Meckel's cartilage; tc, trabeculae cranii.

diagonally as in controls. The muscles often are fused with each other (Fig. 5A,F). However, the muscle anlagen appear in their normal positions. The mm. levator mandibulae longus profundus et internus, which normally detach themselves from the m. levator mandibulae longus superficialis during myogenic cell differentiation around Stage 40, do so late and incompletely, and the muscle fibres differentiate in close proximity to m. levator mandibulae longus superficialis (Fig. 4E,F). The m. levator mandibulae articularis, which normally develops separated from the m. levator mandibulae longus superficialis, fuses to this muscle. All muscles are frayed at their insertion. Also, only some individual muscle fibres, instead of a compact muscle, insert at Meckel's cartilage, a consequence of incomplete initial myotube formation and maturation. During rostral extension, the muscles follow the cartilage anatomy and elongate in a swerved fashion toward Meckel's cartilage. The m. levator mandibulae externus could not be identified in all embryos, probably owing to its late development (Tables 2 and 3). The m. intermandibularis also is affected on the uninjected side and the muscle appears frayed along its entire length (Fig. 5B). The muscle anlagen differentiate as a loose cell cluster and the contralateral muscles are fused incompletely.

Hyoid arch musculature

The three bilateral hyoid arch muscles innervated by cranial nerve VII (Edgeworth, 1935) are formed late in development (Fig. 4K,L): the quadratohyoangularis, the orbitohyoideus and the interhyoideus. The m. quadratohyoangularis, which normally connects Meckel's cartilage with the palatoquadrate, supports the opening of the mouth by depressing Meckel's cartilage. In FoxN3-depleted tadpoles, the muscle does not extend all the way to Meckel's cartilage and the tadpoles could not open their mouths (Fig. 3C). The anlage of the hyoid muscle plate is located caudal to the mandibular muscle plate and has the normal separation into three distinct portions. Later, during myogenic cell differentiation, the m. quadratohyoangularis anlage does not extend ventrally to a more cranial insertion and the insertion remains at the palatoquadrate cartilage (Fig. 4G,H). The origin shifts, with some delay, to a more ventral position at the palatoquadrate, just as on the control side. Furthermore, the muscle anastomoses at the origin with the m. orbitohyoideus, which is enlarged. The m. interhyoideus, which normally forms as a thin curved muscle between the ceratohyal cartilages, is thickened and originates on the entire median surface of the ceratohyal, instead of from the ventral margin (Fig. 3D). During proliferation, there are more myoblasts than on the control side. Moreover, the cell
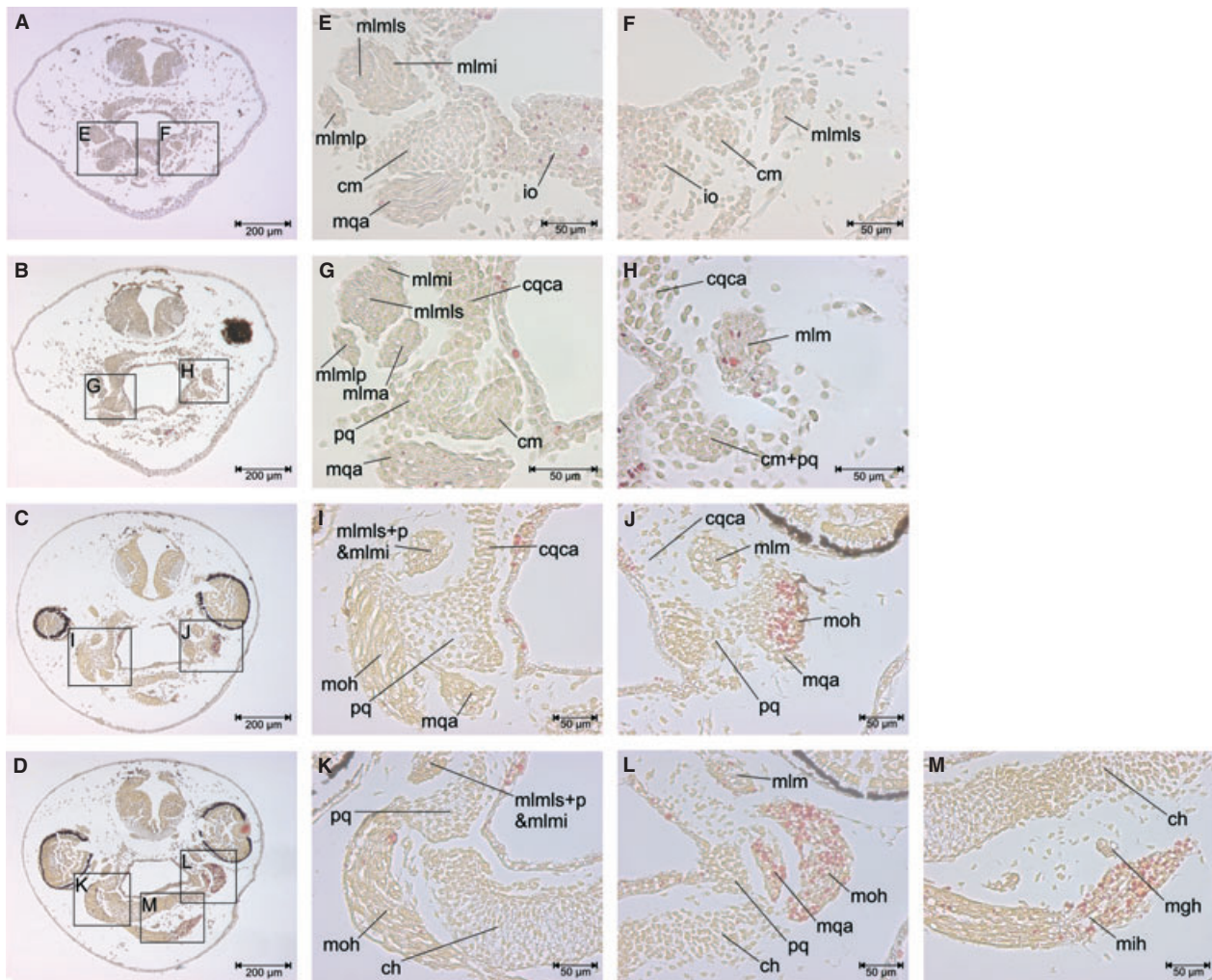
Fig. 4 Transverse sections of a unilaterally FoxN3-MO-injected *X. laevis* larva at Stage 42. (E–M) Enlargements of areas indicated in A–D, which are transverse sections through the mandibular and hyoid muscle regions. The cartilage and muscle development is delayed by two stages at the injected (right) side compared to the control (left) side. Functional knockdown of FoxN3 leads to a delay in NC-derived cartilages and cranial muscle differentiation. At the control side the first muscle fibres are already differentiated, whereas the injected side still has only myoblasts. Furthermore, cartilage precursors condense in their proper position but differentiate incompletely on the injected side compared to the control side. ch, ceratohyal; cm, Meckel's cartilage; cqca, commisura quadratocranialis anterior; io, infrarostral; mgh, m. geniohyoideus; mih, m. interhyoideus; mlmi, m. levator mandibulae inferior; mlma, m. levator mandibulae anterior; mlmlp, m. levator mandibulae longus profundus; mlmls, m. levator mandibulae longus superior; moh, m. orbitohyoideus; pq, palatoquadrate.

alignment to the midline, when cell division stops, is disordered such that the entire muscle appears frayed (Fig. 4M).

Branchial arch musculature

The 10 branchial arch muscles support the filigreed structure of the gill basket necessary for filter feeding, through the stabilisation, extension and compression of the gill basket. The development of most branchial arch muscles is delayed, but takes place in the normal positions. However, the levator and depressor muscles are fragmented and disordered (Fig. 5C,D). During development, no consistent muscle anlagen of the mm. levator arcuum branchialium

are formed and the muscles, which normally cover the branchial basket dorsolaterally, only extend over about half of the gill basket and cover the branchial basket incompletely. Moreover, the cell alignment during muscle differentiation is disordered. The levator and depressor muscles are smaller than on the uninjected side and in control tadpoles; this probably is correlated with the shortened gill basket (Fig. 3F). The m. subcularis rectus I was anastomosed with the m. geniohyoideus at the origin (Fig. 5E). The cellular anlage of the m. subcularis rectus I is smaller than in controls and does not shift to a more dorsomedial position as it develops. It also fused with the cellular anlage of the m. geniohyoideus. Most of the m. transversus ventralis II

Table 1 Summary of the malformations of mandibular (man), hyoid (hyo), branchial (bra) and hypobranchial (hyp) muscles found after uni- or bilateral FoxN3-MO injection. The nomenclature follows Ziermann & Olsson (2007) and the abbreviations are the same as those used in the figures.

Name	Control specimens		Morpholino injected specimens	
M. levator mandibulae longus group; mlml (man)	O:	Arcus subocularis (palatoquadrate cartilage)	O:	Arcus subocularis (palatoquadrate cartilage)
	I:	Superficialis portion: Meckel's cartilage, profundus portion: extends into soft tissue, internus portion: Processus articularis (Meckel's cartilage)	I:	Superficialis portion: Meckel's cartilage, profundus portion: extends into soft tissue, internus portion: Processus articularis (Meckel's cartilage) – shifted to ventral position
	C:	Splits cranially into three separated muscle bundles, superficialis, profundus and internus portion, nearly horizontal progression to insertion	C:	Splits cranially incompletely into partly fused superficial, profundus and internus portions, bent progression to insertion
M. levator mandibulae articularis; mlma (man)	O:	Processus muscularis (palatoquadrate cartilage)	O:	Processus muscularis (palatoquadrate cartilage)
	I:	Processus retroarticularis (Meckel's cartilage)	I:	Processus retroarticularis (Meckel's cartilage)
	C:	Runs horizontally to attach on medial region of Meckel's cartilage	C:	Short, runs cranially, bent towards the insertion and does not reach medial region of Meckel's cartilage
M. levator mandibulae externus; mlme (man)	O:	Processus articularis (palatoquadrate cartilage)	O:	Processus articularis (palatoquadrate cartilage)
	I:	Meckel's cartilage (dorsolaterally)	I:	Meckel's cartilage on opposite side of the body (ventrolaterally)
M. intermandibularis; mim (man)	O:	Meckel's cartilage	O:	Meckel's cartilage
	I:	Contralateral counterpart fuses medially	I:	Contralateral counterpart fuses incompletely
			C:	Entire muscle with disordered and frayed appearance, curvature caudally stretched
M. orbitohyoideus; moh (hyo)	O:	Processus muscularis (palatoquadrate cartilage)	O:	Processus muscularis (palatoquadrate cartilage)
	I:	Ceratohyal cartilage	I:	Ceratohyal cartilage
			C:	Caudally at the processus lateralis hyalis, small, disordered and frayed
M. quadratohyoangularis; mqh (hyo)	O:	Processus muscularis (palatoquadrate cartilage)	O:	Processus muscularis (palatoquadrate cartilage)
	I:	Meckel's cartilage	I:	Processus muscularis (palatoquadrate cartilage)
	C:	Connects processus muscularis to Meckel's cartilage	C:	Forms a thick muscle ventral to the palatoquadrate cartilage
M. interhyoideus; mih (hyo)	O:	Ceratohyal cartilage	O:	Ceratohyal cartilage
	I:	Contralateral counterpart fuses medially	I:	Contralateral counterpart fuses incompletely
	C:	Planar, slender curvature ventral to ceratohyal cartilage	C:	Short, wide, disordered and frayed curvature ventral to the ceratohyal cartilage
M. subarcularis rectus I; msr I (bra)	O:	Ceratobranchial cartilage I (proximal)	O:	Ceratobranchial cartilage I (proximal)

Table 1 (Continued).

Name	Control specimens		Morpholino injected specimens	
	I:	Processus posterior hyalis (ceratohyal cartilage)	*I:*	Processus posterior hyalis (ceratohyal cartilage)
	C:	Orginates rostral to m. geniohyoideus	*C:*	Fused at the origin with the m. geniohyoideus
M. transversus anterior; mta (bra)	*O:*	Planum hypobranchiale	*O:*	Planum hypobranchiale
	I:	Basihypobranchiale	*I:*	Extends into soft tissue, lateral to basihypobranchiale
M. transversus ventralis II; mtv II (bra)	*O:*	Ceratobranchial cartilage II	*O:*	Ceratobranchial cartilage II
	I:	Fuses medially with contralateral counterpart	*I:*	Fuses medially with contralateral counterpart
	C:	Slender curvature ventral to the ceratobranchial cartilage II	*C:*	Disordered and frayed curvature ventral to the ceratobranchial cartilages II and III
Mm. levatores arcuum branchialium I–IV; mlab I–IV (bra)	*O:*	Portion I: processus ascendens palatoquadrati (palatoquadrate cartilage) portion II–IV: Crista parotica (capsula auditiva)	*O:*	Portion I: processus ascendens palatoquadrati (palatoquadrate cartilage) portion II–IV: Crista parotica (capsula auditiva)
	I:	Ceratobranchial cartilage and commisura terminalis, respectively	*I:*	Ceratobranchial cartilage and commisura terminalis, respectively
	C:	Compact array of muscles	*C:*	Interrupted and frayed array of muscles
Mm. constrictores branchiales II–IV; mcb II–IV (bra)	*O:*	At the respective commisura terminalis (ceratobranchial cartilage)	*O:*	At the respective commisura terminalis (ceratobranchial cartilage)
	I:	At the respective ceratobranchial cartilage	*I:*	At the respective ceratobranchial cartilage
	C:	Thin muscles ventral to the branchial basket	*C:*	Frayed and disordered muscles ventral to the branchial basket
M. geniohyoideus; mgh (hyp)	*O:*	Ceratobranchial cartilage I (proximal)	*O:*	Ceratobranchial cartilage I (proximal)
	I:	Infrarostral cartilage	*I:*	Meckel's cartilage
	C:	Originate caudal to m. subcularis rectus I	*C:*	Fused at origin with the m. subcularis rectus I, smaller and shorter
M. rectus cervicis; mrc (hyp)	*O:*	Abdominal wall, as rostral sequel to the m. rectus abdominalis	*O:*	Abdominal wall, as rostral sequel to the m. rectus abdominalis
	I:	Ceratobranchial cartilage III and commisura proximalis III	*I:*	Ceratobranchial cartilage III and commisura proximalis III
			C:	Frayed and disordered appearance

O, origin; *I*, insertion; *C*, characteristics.

appears frayed over its entire extension and is broadened (Fig. 5E). As in the cellular anlagen of the m. interhyoideus and m. intermandibularis, more myoblasts are formed during proliferation than on the uninjected side, and myotube formation is incomplete. Furthermore, the cellular anlage switches to a more caudal position on the third ceratobranchial instead of the second ceratobranchial.

Hypobranchial musculature

Tadpoles of *X. laevis* have two hypobranchial muscles – the m. geniohyoideus (Weisz, 1945) and the m. rectus cervicis (Sokol, 1977; m. sternohyoideus). Like the other three muscle groups, the hypobranchial muscles developed in their normal positions. The m. geniohyoideus was missing in two bilateral and one unilateral FoxN3-knockdown tadpole (Fig. 3E). In the rest, it was shortened and anastomosed at its origin with the m. subcularis rectus I (Fig. 5E). During development, the muscle anlage normally extends from the cranial margin of the gill basket to the infrarostral cartilage. In the FoxN3-depleted tadpoles the development was delayed and the anlage extended to the level of Meckel's cartilage or the

Fig. 5 Three-dimensional reconstruction of the skull and cranial muscles of an unilaterally FoxN3-MO-injected *Xenopus laevis* larva at Stage 46 in frontal (A,B), lateral (C,D), ventral (E) and dorsal (F) view. Functional knockdown of FoxN3 produced a wide variety of muscle malformations, such as frayed and disordered appearance (mlab), shifts of insertions (mqh) and anastomoses (mgh + msrI). The muscles are smaller and show an aberrant course on the injected compared to the control side. mcb II–IV, mm. constrictores branchiales II–IV; mcl-dv, m. constrictores laryngis dorsalis et ventralis; mdl, m. dilator laryngis; mgh, m. geniohyoideus; mih, m. interhyoideus; mim, m. intermandibularis; mlab I–IV, mm. levator arcuum branchialium I–IV; mlme, m. levator mandibulae externus; mlmi, m. levator mandibulae inferior; mlma, m. levator mandibulae anterior; mlmlp, m. levator mandibulae longus profundus; mlmls, m. levator mandibulae longus superior; moi, m. obliquus inferior; moh, m. orbitohyoideus; mos, m. obliquus superior; mra, m. rectus anterior; mri, m. rectus inferior; mrp, m. rectus posterior; mrs, m. rectus superior; msr I, m. subarcualis rectus I; mta, m. transversus anterior; mtv II, m. transversus II.

Table 2 Timing of the development of the mandibular (man), hyoid (hyo), branchial (bra) and hypobranchial (hyp) head muscles in control tadpoles. The nomenclature follows that of Ziermann & Olsson (2007) and larval stages are those of Nieuwkoop & Faber (1994).

	Stage										
Muscle	36	37	38	39	40	41	42	43	44	45	46
M. levator mandibulae longus internus; mlmli (man)											
M. levator mandibulae longus profundus; mlmlp (man)				?							
M. levator mandibulae longus superior; mlmls (man)											
M. levator mandibulae articularis; mlma (man)											
M. levator mandibulae externus; mime (man)											
M. intermandibularis; mim (man)											
M. quadrato-hyoangularis; mqh (hyo)											
M. orbitohyoideus; moh (hyo)											
M. interhyoideus; mih (hyo)											
M. subarcualis rectus I; msr I (bra)											
M. transversus anterior; mta (bra)											
M. transversus ventralis II; mtv II (bra)											
Mm. levator arcuum branchialium I–IV; mlab I–IV (bra)											
Mm. constrictores branchialium II–IV; mcb II–V (bra)											
M. geniohyoideus; mgh (hyp)											
M. rectus cervicis; mrc (hyp)											

The abbreviations are the same as those used in the figures. Code to colours of table cells: white = no apparent muscle anlagen; light grey = mesodermal cell cluster; medium grey = myoblasts; dark grey = fibre development; black = muscle. A question mark indicates that an earlier appearance of an anlage could not be excluded.

Table 3 Timing of head muscle development of the mandibular (man), hyoid (hyo), branchial (bra) and hypobranchial (hyp) muscles in FoxN3-depleted tadpoles. The nomenclature follows that of Ziermann & Olsson (2007) and larval stages are those of Nieuwkoop & Faber (1994).

	Stage										
Muscle	36	37	38	39	40	41	42	43	44	45	46
M. levator mandibulae longus internus; mlmli (man)											
M. levator mandibulae longus profundus; mlmlp (man)				?							
M. levator mandibulae longus superior; mlmls (man)											
M. levator mandibulae articularis; mlma (man)				?							
M. levator mandibulae externus; mime (man)											
M. intermandibularis; mim (man)											
M. quadrato-hyoangularis; mqh (hyo)											
M. orbitohyoideus; moh (hyo)											
M. interhyoideus; mih (hyo)											
M. subarcualis rectus I; msr I (bra)											
M. transversus anterior; mta (bra)					?						
M. transversus ventralis II; mtv II (bra)											
Mm. levator arcuum branchialium I–IV; mlab I–IV (bra)											
Mm. constrictores branchialium II–IV; mcb II–IV (bra)											
M. geniohyoideus; mgh (hyp)											
M. rectus cervicis; mrc (hyp)											

The abbreviations are the same as those used in the figures. Code to colours of table cells: white = no apparent muscle anlagen; light grey = mesodermal cell cluster; medium grey = myoblasts; dark grey = fibre development; black = muscle. A question mark indicates that an earlier appearance of an anlage could not be excluded.

ceratohyal cartilage. Moreover, the cellular anlage was much smaller in contrast to the uninjected side or in control animals. Like the m. geniohyoideus, the m. rectus cervicis appeared frayed and it origin was shifted to a more caudal position than that of the muscle on the control side (Fig. 5D,E). The cell alignment and myotube

formation was disordered, such that both muscles appeared frayed over their entire extension.

Discussion

Our results provide direct evidence that FoxN3 is essential for cranial NC development in *Xenopus laevis*, and indicate a role for FoxN3 in the evolution of novel cartilages unique to frog larvae, such as the rostral cartilages and the specialised gill basket. The role of FoxN3 during development of muscle and cartilage formation was investigated using a FoxN3-MO. Embryos that were morpholino-injected at the two-cell stage had a normal pattern of early cartilage and muscle anlagen, except for the anlagen of the infrarostral and Meckel's cartilage. In subsequent stages, we found less increase in size and an abnormal muscle and cartilage formation emerging from Stage 38 onwards. This indicates a role for FoxN3 in the differentiation of NC-derived chondrocyte lineages and in muscle morphogenesis. Additionally, because of loss of articulations between NC-derived cartilages, FoxN3 was shown to play a prominent role in joint development and in the formation of the infrarostral cartilage.

Defining the role for FoxN3 in the evolution of rostral cartilages

From an evolutionary perspective, it is important to note that most malformations caused by FoxN3 depletion affect innovations unique to anuran tadpoles, i.e. the filigreed structure of the gill basket (that functions as a filter) and the rostral cartilages (infra- and suprarostrals). Interestingly, the simplified gill basket in FoxN3-depleted *Xenopus* larvae resembles homologous structures in salamanders such as the axolotl (*Ambystoma mexicanum*). The rostral cartilages, which do not exist in salamander larvae, were small and malformed in the experimental tadpoles. Evolutionary changes, either modifying existing morphological structures or generating new ones, may result from variation in genetic control. The mesenchymal anlagen of the infrarostral and Meckel's cartilage were the only anlagen that developed in an incorrect position, having been shifted to a more central position. During further development, the anlagen rested against each other and the infrarostral was a broadened and ventrally elongated cartilage. The suprarostral plate was completely developed by Stage 46 in control specimens, but in FoxN3-depleted tadpoles the suprarostral plate was not visible at this stage; however, it cannot be excluded that it might have been formed later, had the FoxN3-depleted tadpoles not died around Stage 48. Nonetheless, the malformation of the infrarostral cartilage indicates that FoxN3 is involved in the patterning of the rostral cartilages. Several genes have been discussed in the context of their origin, such as *Dlx*, *BMP* and *bagpipe* genes, and genes related to jaw development (Svensson &

Haas, 2005). Functional knockdown of FoxN3 led to a decrease in the expression of different *Nkx 3.2* genes such as *Xbap* and *zax* in the infrarostral and Meckel's cartilages (Schuff et al. 2007). Additionally, FoxN3 depletion resulted in incorrect formation of the jaw joint. Our study together with data from previous studies suggests that FoxN3 may be important for the developmental process underlying the origin of the infrarostral and maybe also the suprarostral cartilage.

FoxN3 is required for neural crest-derived cartilage development

The only cranial cartilage elements affected following functional knockdown of FoxN3 were those that were NC-derived; the basihyal and the plana hypobranchiale were normal. Furthermore, the otic capsules and the parachordals also showed normal development. Classical extirpation experiments in the axolotl have shown that despite the loss of NC cells, the basihypobranchial, the parachordals, and the otic capsules are normal, which prompted Hörstadius & Sellman (1946) to suggest that these elements are mesodermal in origin. Early studies by Stone in the 1920s (Stone, 1926), as well as more recent studies in the Oriental fire-bellied toad (*Bombina orientalis*), have come to similar conclusions and suggest that this a common feature for anurans (Sadaghiani & Thiebaud, 1987; Olsson & Hanken, 1996). We propose that FoxN3 has an exclusive role in the development of NC-derived cartilages. Neural crest-derived mesenchyme is not equivalent to mesenchyme of mesodermal origin with regard to its ability to respond to FoxN3 signals (Schuff et al. 2007; Samaan et al. 2010). This suggests that NC-derived mesenchyme requires distinct signals for correct development that mesoderm-derived mesenchyme cells do not require. The mesoderm-derived cartilages (basihyal, basibranchial and otic capsule) end up in a false position, but this seems to be caused by the smaller size and malformation of the NC-derived cartilages. In contrast to these results, experiments on the development of the head in chickens have shown that NC cells can act like mesoderm cells, and that morphogenetic processes that pattern the cranial skeleton do not discriminate between the two cell lineages (Schneider, 1999). The transplantation experiments using quail NC cells transplanted into chicken embryos demonstrated the ability of NC cells to pattern cartilages that are morphologically indistinguishable from mesodermally derived elements, but whether mesoderm cells can replace NC cells remains unknown. We interpret our results as support for a neural crest-specific effect of FoxN3 in normal *X. laevis* development, and as suggesting that NC and mesoderm cells in late stages (FoxN3 starts to have visible effects at Stage 39) are differentiated enough to react quite differently to FoxN3 knockdown. Schneider's (1999) results might reflect that the NC cells used were at an early stage

of differentiation and were more responsive to signals from surrounding tissues.

FoxN3 did not affect the migration pattern of NC cells into the branchial arches (Schuff et al. 2007), but FoxN3-depleted tadpoles had reduced sizes of all NC-derived cranial cartilages in contrast to control tadpoles and, during pre-cartilage condensation, the aggregation and differentiation of the NC-derived chondrocyte lineages was delayed. Grüneberg (1963) named the early initial phase of skeletal development 'membranous skeleton'. Different mechanisms for the condensation of the membranous skeleton are known for different tissue types, but little is known about the mechanisms during formation of the NC-derived chondrocyte lineage (Hall & Miyake, 1992; Hall, 2005). In amphibians, the preconditions for cartilage formation of the NC-derived chondrocyte lineage are mainly related to the ectomesenchyme–endoderm interaction system, whereas mitotic cell division is responsible for the spread of inductive signals (Epperlein & Lehmann, 1975; Seufert & Hall, 1990). The anlagen of the cartilages appeared as loose mesenchyme cell clusters in the position of the prospective cranial cartilages in FoxN3-depleted and control tadpoles at Stage 38. Later the condensation of the NC-derived chondrocyte lineage was delayed by two stages in FoxN3-depleted larvae. In controls, the prechondroblasts aggregated in Stage 40, but in FoxN3-depleted larvae they did not appear as distinct condensations until Stage 42. In the subsequent stages, chondroblast formation and the chondrocyte differentiation were also delayed by two stages. This result implies that FoxN3 is necessary for the early inductive signals of chondrogenesis, mainly for the aggregation, because chondroblasts and later chondrocytes differentiate during the same time period as in the control tadpoles.

Additionally, a smaller number of cells aggregated in the anlagen and the sizes of the individual anlagen were reduced. The most distinctive feature, however, was the loss of skeletal processes in FoxN3-depleted tadpoles. The processes were formed as outgrowths on existing cartilage condensations. A minimal mesenchymal cell number was necessary for the initiation of chondrogenesis and a reduced size of the anlagen gave rise to smaller cartilages or none at all (Hall & Miyake, 1992). During prechondrogenic condensation, larger condensations retained their compact cores, whereas smaller ones spread out and lost their compact character (Umansky, 1966). The phocomelia mutation in *Mus musculus* leads to a 24-h delay in condensation, and even if the condensation finally reached normal size the maxilla and the mandible were smaller (Hall & Miyake, 1992). Apparently the delay in timing caused this malformation, as too few cells were available at the time when the anlagen of maxilla and mandible were formed. It seems that functional knockdown of FoxN3 leads to a smaller number of cells in the anlagen, which leads to smaller sizes or even complete loss of cranial cartilages because the membranous skeleton cannot form properly. We propose that, if an insufficient number of cells aggregate, they cannot differentiate into cartilage processes, and are instead incorporated into the cartilage body.

The delayed aggregation and the smaller size of the prechondrogenic condensation are both examples of incorrect processes of aggregation of the membranous skeleton. FoxN3 has been shown to act as a cell cycle checkpoint suppressor (Ches1) in a screen of factors that are able to restore damage-induced G (2)/M arrest in checkpoint-deficient strains of *Saccharomyces cerevisiae* (Pati et al. 1997). Prechondrogenic cells are characterised by high rates of cell division, the formation of gap junctions that facilitate intercellular communications, and a change in the type of glycosaminoglycans secreted by the cells. In Talpid, a mutant of domestic chicken, the duration of both the G1 and S phases of the chondrogenic cell cycle was affected, which led to more adhesive, less motile cells and an inability to produce correctly oriented growth plates (Hall & Miyake, 1992). Therefore, we assume that the incorrect and delayed aggregation is based on a disordered cell cycle and a lack of appropriate inductive signals. This may be mediated by a decrease or slowing down of cell cycle progression or an increase in apoptotic cells during the cell cycle. FoxN3 knockdown in *X. laevis* led to a reduction in eye size and loss of structures mediated by an increase of apoptotic cells of about 60% (Schuff et al. 2007). Moreover, human and *X. laevis* FoxN3 bound Sin3 and Rpd3, components of the histone deacetylase complex (Scott & Plon, 2003; Schuff et al. 2007). The histone deacetylase complex regulated cell processes by recruiting transcription factors, which mediated transcriptional repression of target genes (Ayer, 1999). In zebrafish (*Danio rerio*), injections of a *hadc-1* morpholino oligonucleotide led to a complete absence of neural crest-derived cartilages, but the mesoderm-derived cartilages were formed (Pillai et al. 2004). Additionally, HDAC inhibitors led to a cessation of growth, premature differentiation, and an increase of apoptosis, due to activation of cyclin-dependent kinase inhibitor p21 (Marks et al. 2001; Minucci & Pelicci, 2006). Although the effect of functional knockdown on NC-derived cartilages has been documented, further research is required to define the signalling cascade in which FoxN3 is embedded. This makes it possible to define the differences that have evolved in the FoxN3 pathway, and to investigate their role in the evolution of morphological novelties, by comparison with salamander species such as the axolotl.

FoxN3 is required for cranial muscle morphogenesis

The malformations of the cranial muscles caused by FoxN3 knockdown resemble the malformations observed following NC cell extirpation (Hall, 1950; Olsson et al. 2001; Ericsson & Olsson, 2004). In FoxN3-depleted tadpoles and following NC extirpation, muscles started to differentiate at

their normal origins but failed to extend towards their insertions, and their fibres were incompletely developed. Only the mandibular, hyoid and branchial muscles developed abnormally; the muscles of the larynx and most of the ocular muscles were not affected by functional knockdown of FoxN3. The connective tissue of the affected muscles is NC-derived, whereas the connective tissue of the larynx muscles is derived from lateral plate mesoderm and the muscles from the cranial-most somites (Piatt, 1938; Noden, 1983a; Piekarski & Olsson, 2007). The ocular muscles formed a developmental module that was relatively independent of other branchial muscles, and their developmental timing was variable among species (Ericsson et al. 2009). The effects on their origin and insertion by functional knockdown of FoxN3 are probably indirectly caused by the delayed development and the malformations of cranial cartilages.

NC cells contributed to the connective tissue surrounding visceral arch muscles and attaching muscles to cartilages (Sadaghiani & Thiebaud, 1987; Olsson et al. 2001; Ericsson et al. 2004). Throughout migration, pattern formation and histogenesis, the positional relation is maintained among hindbrain segments, neural crest, and musculoskeletal derivatives (Graham et al. 1996; Koentges & Lumsden, 1996; Schilling & Kimmel, 1997; Graham & Smith, 2001; Olsson et al. 2001). This results, for example, in the connective tissue components of a given muscle and its skeletal attachment site(s) being derived from the same migratory crest stream. The muscle anlagen of all cranial muscles were formed in the correct positions close to their future origins, but the sizes of the anlagen were reduced in FoxN3-depleted tadpoles in contrast to the controls. All muscles appeared frayed at their insertions, and were shortened. Muscle shape and size were defined by the surrounding NC cells and NC-derived cartilages (Rinon et al. 2007; Tokita & Schneider, 2009). Cell differentiation in the mesodermal anlagen was regulated through an enhanced cell proliferation of NC cells. Additionally, myogenesis was also maintained by NC cells through segregation of BMP antagonists such as gremlin or chordin (Noden & Francis-West, 2006). Therefore, the smaller size of the muscle anlagen and the shortened muscles in FoxN3-depleted tadpoles might be caused indirectly by improper development of NC-derived cells. Further genetic investigations are necessary to identify the affected part of myogenesis. However, the anlagen are formed in the correct position and, therefore, a proper migration of cranial paraxial mesoderm cells seems to have taken place.

The normal spatial and temporal pattern of cranial muscle differentiation in *X. laevis* has been documented (Ziermann & Olsson, 2007). In contrast, in FoxN3-depleted tadpoles, muscle differentiation is delayed by two stages, just as in the development of the cartilages. The development of some cranial muscles was closely correlated with the chondrification of the skeletal tissue (McClearn & Noden, 1988).

The muscle anlagen normally became separated from each other, when cells from the surrounding connective tissues migrated into the anlage. The m. geniohyoideus was fused to the m. subarcualis rectus I at their origin in FoxN3-depleted tadpoles, but in the control tadpoles the m. geniohyoideus originated at the ceratobranchial I, caudal to the m. subarcualis rectus I. During development, the anlagen normally separated from each other through the development of the ceratobranchial cartilage (Ziermann & Olsson, 2007). Following functional knockdown, the ceratobranchials were malformed and the branchial basket reduced in size. The anlagen failed to separate because apparently no connective tissue migrated into anlagen to separate them. Subsequently, the muscles developed in a cranial to caudal direction, but unlike the controls, fibre development was not complete when they reached their insertions. The myoblasts within the muscle anlagen were disordered and formed a loose assembly. During normal muscle fibre differentiation, the myoblasts line up in a series to form cell–cell contacts and multicellular muscle fibres (Gilbert & Singer, 2006). The myoblasts in FoxN3-depleted tadpoles formed a loose connection during cranial muscle development and muscle fibres later tended to separate from each other, giving the muscles a frayed appearance. Furthermore, the anlage of the m. quadrato-hyoangularis did not extend to its normal insertion at Meckel's cartilage, but remained at the palatoquadrate cartilage. The NC-derived connective tissues surrounding the myofibres provided directional guidance during muscle development (Ericsson et al. 2004). It is therefore logical to interpret the poor differentiation of the muscles as an indirect effect of the deficiencies and irregularities of the cartilage development.

The evolution of the jaw joint

The processes leading to the formation of the jaw at the transition between agnathans and gnathostomes are not well understood. Comparisons of the two groups have shown that no simple remodelling of pre-existing structures has occurred (Shigetani et al. 2002). The oral structures are formed by distinct cell lineages, and the epithelial–mesenchymal interactions, as well as the expression patterns of orthologous genes, have changed during evolution. Therefore, the gnathostome jaw should be seen as a novelty (Kuratani, 2004, 2005). Despite the different functions of the gnathostome jaw region (e.g. mastication or hearing), it has been shown that the genetic control is highly conserved for the primary jaw structures. One of these conserved genes is the *Nkx3.2* gene. The homologues have been cloned from zebrafish, *Xenopus*, chick, mice and human. (Newman et al. 1997; Tribioli & Lufkin, 1997; Tribioli et al. 1997; Miller et al. 2003; Wilson & Tucker, 2004). The developmental role of the *Nkx3.2* gene in the development of the jaw joint in *X. laevis* is shared with chicken and zebrafish. *Nkx3.2* is expressed in both palatoquadrate and

Meckel's cartilages (Newman et al. 1997). In the lamprey, a homologue of *Nkx3.2* is also known, but no expression in the pharyngeal arches has been documented (Kuraku et al. 2010). *Nkx3.2* depletion leads to fusion of the jaw joint and a loss of the retroarticular process of Meckel's cartilage in zebrafish and the chicken (Miller et al. 2003; Wilson & Tucker, 2004). Svensson & Haas (2005) have suggested that *Nkx3.2*, and its paralogue *Nkx3.3*, might be important for the evolution of novel joints such as the one between the infrarostral and Meckel's cartilages. A decrease in *Nkx 3.2* expression, such as *Xbap* (Newman et al. 1997) in Meckel's cartilage, or of the paralogue *Nkx3.3*, such as *zax* (Newman & Krieg, 1999) in the infrarostral cartilage, as well as the loss of all articulations in the larval head of *X. laevis*, indicates that FoxN3 should be viewed as another gene required for correct jaw formation and for the formation of new articulations. Following FoxN3 knockdown, all articulations were lost, the jaw articulation, the articulation between the infrarostral and Meckel's cartilage, and the movable articulation between the ceratohyal cartilages. Most of our knowledge of the mechanisms and processes of joint formation has been gained from studies of limb development and the mammalian (secondary) jaw joint. These studies have shown that a first phase of jaw development produces cartilaginous anlagen and the interzone in which the joint will develop, and that the joint cavity develops later in a second phase (Pitsillides & Ashhurst, 2008). The jaw joint in *X. laevis* is formed between the anlagen of Meckel's cartilage and the palatoquadrate, which emerge from the same anlage (Cerny et al. 2004). In both FoxN3-depleted tadpoles and controls, these cartilages were formed as separate, discrete entities, but following FoxN3 knockdown, no intervening zone was formed. The same was observed between the ceratohyal cartilages and between infrarostral and Meckel's cartilages. The similarities between Nkx3.2 and FoxN3 depletion may indicate a role for FoxN3 in bagpipe regulation, but this needs further investigation. The function of FoxN3 suggests a role in joint development of *X. laevis* and that it may have acquired an additional developmental role in directing the formation of a novel joint between the infrarostral and Meckel's cartilages. Further analyses are needed to test whether FoxN3 acts in an evolutionarily conserved manner in gnathostome jaw joint development.

Concluding remarks

Our findings indicate that FoxN3 is important for the development of novel cartilages in the oral apparatus of the pipid frog *X. laevis*. Morpholino knockdown of FoxN3 leads to atavisms, conditions similar to the less specialised condition seen in salamanders, i.e. the gill basket is much simplified, and there are no rostralia, at least not as free cartilage elements. Moreover, we show that FoxN3 is essential for cranial NC-derived cartilage development and, probably indirectly,

for cranial muscle patterning. FoxN3 might acts as a cell cycle regulator during mesenchyme condensation. We are in the process of identifying further target genes of FoxN3 to gain a deeper understanding of the developmental processes active during chondrogenesis and muscle patterning in amphibian head development. Little is known about the development of cranial articulations, and we will analyse jaw joint-specifying genes to get insights into how these novel structures, unique to anuran tadpoles, have evolved.

References

Ayer DE (1999) Histone deacetylases: transcriptional repression with SINers and NuRDs. *Trends Cell Biol* **9**, 193–198.

Barembaum M, Bronner-Fraser M (2005) Early steps in neural crest specification. *Semin Cell Dev Biol* **16**, 642–646.

Böck P (ed.) (1989) *Romeis Mikroskopische Technik*. Munich: Urban & Schwarzenberg.

Cerny R, Lwigale P, Ericsson R, et al. (2004) Developmental origins and evolution of jaws: new interpretation of 'maxillary' and 'mandibular'. *Dev Biol* **276**, 225–236.

Couly GF, Coltey PM, Ledouarin NM (1992) The developmental fate of the cephalic mesoderm in quail-chick chimeras. *Development* **114**, 1–15.

De Sa RO, Swart CC (1999) Development of the suprarostral plate of pipoid frogs. *J Morphol* **240**, 143–153.

Dottori M, Gross MK, Labosky P, et al. (2001) The winged-helix transcription factor Foxd3 suppresses interneuron differentiation and promotes neural crest cell fate. *Development* **128**, 4127–4138.

Edgeworth FH (1935) *The Cranial Muscles of Vertebrates*. London: Cambridge University Press.

Epperlein HH, Lehmann R (1975) Ectomesenchymal–endodermal interaction system (EEIS) of *Triturus* alpestris in tissue-culture 2. Observations on differentiation of visceral cartilage. *Differentiation* **4**, 159–174.

Ericsson R, Olsson L (2004) Patterns of spatial and temporal visceral arch muscle development in the Mexican axolotl (*Ambystoma mexicanum*). *J Morphol* **261**, 131–140.

Ericsson R, Cerny R, Falck P, et al. (2004) Role of cranial NC cells in visceral arch muscle positioning and morphogenesis in the Mexican axolotl, *Ambystoma mexicanum*. *Dev Dyn* **231**, 237–247.

Ericsson R, Ziermann JM, Piekarski N, et al. (2009) Cell fate and timing in the evolution of neural crest and mesoderm

development in the head region of amphibians and lungfishes. *Acta Zool* **90**, 264–272.

Evans DJR, Noden DM (2006) Spatial relations between avian craniofacial neural crest and paraxial mesoderm cells. *Dev Dyn* **235**, 1310–1325.

Francis-West P, Ladher R, Barlow A, et al. (1998) Signalling interactions during facial development. *Mech Dev* **75**, 3–28.

Gilbert SF, Singer SR (2006) *Developmental Biology*. Sunderland, MA: Sinauer Ass.

Gomez-Skarmeta JL, de la Calle-Mustienes E, Modolell J, et al. (1999) *Xenopus* brain factor-2 controls mesoderm, forebrain and neural crest development. *Mech Dev* **80**, 15–27.

Graham A, Smith A (2001) Patterning the pharyngeal arches. *Bioessays* **23**, 54–61.

Graham A, Koentges G, Lumsden A (1996) NC apoptosis and the establishment of craniofacial pattern: an honorable death. *Mol Cell Neurosci* **8**, 76–83.

Gross JB, Hanken J (2008) Segmentation of the vertebrate skull: neural-crest derivation of adult cartilages in the clawed frog, *Xenopus laevis. Integr Comp Biol* **48**, 681–696.

Grüneberg H (1963) *The Pathology of Development: A Study of Inherited Skeletal Disorders in Animals*. Oxford: Blackwell.

Hall BK (1950) Experimental modification of muscle development in *Ambystoma punctatum. J Exp Zool* **113**, 355–377.

Hall BK (2005) *Bones & Cartilage: Developmental and Evolutionary Skeletal Biology*. London: Elsevier∕Academic Press.

Hall BK (2009) *The Neural Crest and Neural Crest Cells in Vertebrate Development and Evolution*. New York: Springer-Verlag.

Hall BK, Hörstadius S (1988) *The Neural Crest*. Oxford: Oxford University Press.

Hall BK, Miyake T (1992) The membranous skeleton – the role of cell condensations in vertebrate skeletogenesis. *Anat Embryol* **186**, 107–124.

Hong CS, Saint-Jeannet JP (2005) Sox proteins and neural crest development. *Semin Cell Dev Biol* **16**, 694–703.

Hörstadius S, Sellman S (1946) Experimentelle Untersuchungen über die Determination des knorpeligen Kopfskelettes bei Urodelen. Nova Acta Regiae Societatis Scientiarium Upsaliensis **13**.

Kintner CR, Brockes JP (1984) Monoclonal antibodies identify blastemal cells derived from dedifferentiating muscle in newt limb regeneration. *Nature* **308**, 67–69.

Koentges G, Lumsden A (1996) Rhombencephalic NC segmentation is preserved throughout craniofacial ontogeny. *Development* **122**, 3229–3242.

Kuraku S, Takio Y, Sugahara F, et al. (2010) Evolution of oropharyngeal patterning mechanisms involving Dlx and endothelins in vertebrates. *Dev Biol* **341**, 315–323.

Kuratani S (2004) Evolution of the vertebrate jaw: comparative embryology and molecular developmental biology reveal the factors behind evolutionary novelty. *J Anat* **205**, 335–347.

Kuratani S (2005) Developmental studies of the lamprey and hierarchical evolutionary steps towards the acquisition of the jaw. *J Anat* **207**, 489–499.

Marks PA, Richon VM, Breslow R, et al. (2001) Histone deacetylase inhibitors as new cancer drugs. *Curr Opin Oncol* **13**, 477–483.

Maurus D, Héligon C, Bürger-Schwärzler A, et al. (2005) Noncanonical Wnt-4 signaling and EAF2 are required for eye development in *Xenopus laevis. EMBO J* **2**, 1181–1191.

McClearn D, Noden DM (1988) Ontogeny of architectural complexity in embryonic quail visceral arch muscles. *Am J Anat* **183**, 277–293.

Metscher BD (2009) MicroCT for comparative morphology: simple staining methods allow high-contrast 3D imaging of diverse non-mineralized animal tissues. *BMC Physiol* **9**, 11, doi: 10.1186/1472-6793-9-11.

Miller CT, Yelon D, Stainier DYR, et al. (2003) Two endothelin 1 effectors, hand2 and bapx1, pattern ventral pharyngeal cartilage and the jaw joint. *Development* **130**, 1353–1365.

Minucci S, Pelicci PG (2006) Histone deacetylase inhibitors and the promise of epigenetic (and more) treatments for cancer. *Nat Rev Cancer* **6**, 38–51.

Newman CS, Krieg P (1999) The *Xenopus* bagpipe-related homeobox gene zampogna is expressed in the pharyngeal endoderm and the visceral musculature of the midgut. *Dev Genes Evol* **209**, 132–134.

Newman CS, Grow MW, Cleaver O, et al. (1997) Xbap, a vertebrate gene related to bagpipe, is expressed in developing craniofacial structures and in anterior gut muscle. *Dev Biol* **181**, 223–233.

Nieuwkoop PD, Faber J (1994) *Normal Table of Xenopus laevis* (Daudin) A systematical and Chronological Survey of the Development from the Fertilized Egg till the End of Metamorphosis. New York: Garland Publishing.

Noden DM (1983a) The role of the NC in patterning of avian cranial skeletal, connective, and muscle tissues. *Dev Biol* **96**, 144–165.

Noden DM (1983b) The embryonic origins of avian cephalic and cervical muscles and associated connective tissues. *Am J Anat* **168**, 257–276.

Noden DM, Francis-West P (2006) The differentiation and morphogenesis of craniofacial muscles. *Dev Dyn* **235**, 1194–1218.

Noden DM, Trainor PA (2005) Relations and interactions between cranial mesoderm and neural crest populations. *J Anat* **207**, 575–601.

Olsson L, Hanken J (1996) Cranial neural-crest migration and chondrogenic fate in the oriental fire-bellied toad *Bombina orientalis*: defining the ancestral pattern of head development in anuran amphibians. *J Morphol* **229**, 105–120.

Olsson L, Falck P, Lopez K, et al. (2001) Cranial neural crest cells contribute to connective tissue in cranial muscles in the anuran amphibian, *Bombina orientalis. Dev Biol* **237**, 354–367.

Pati D, Keller C, Groudine M, et al. (1997) Reconstitution of a MEC1-independent checkpoint in yeast by expression of a novel human fork head cDNA. *Mol Cell Biol* **17**, 3037–3046.

Piatt J (1938) Morphogenesis of the cranial muscles of *Ambystoma punctatum. J Morphol* **63**, 531–587.

Piekarski N, Olsson L (2007) Muscular derivatives of the cranialmost somites revealed by long-term fate mapping in the Mexican axolotl (*Ambystoma mexicanum*). *Evol Dev* **9**, 566–578.

Pillai R, Coverdale LE, Dubey G, et al. (2004) Histone deacetylase 1 (HDAC-1) required for the normal formation of craniofacial cartilage and pectoral fins of the zebrafish. *Dev Dyn* **231**, 647–654.

Pitsillides AA, Ashhurst DE (2008) A critical evaluation of specific aspects of joint development. *Dev Dyn* **237**, 2284–2294.

Rinon A, Lazar S, Marshall H, et al. (2007) Cranial neural crest cells regulate head muscle patterning and differentiation during vertebrate embryogenesis. *Development* **134**, 3065–3075.

Sadaghiani B, Thiebaud CH (1987) Neural crest development in the *Xenopus laevis* embryo, studied by interspecific transplantation and scanning electron microscopy. *Dev Biol* **124**, 91–110.

Samaan G, Yugo D, Rajagopalan S, et al. (2010) *Foxn3* is essential for craniofacial development in mice and a putative candidate involved in human congenital craniofacial defects. *Biochem Biophys Res Commun* **400**, 60–65.

Santagati F, Rijli FM (2003) Cranial neural crest and the building of the vertebrate head. *Nat Rev Neurosci* **4**, 806–818.

Sato T, Sasai N, Sasai Y (2005) Neural crest determination by co-activation of Pax3 and Zic1 genes in *Xenopus* ectoderm. *Development* **132**, 2355–2363.

Schilling TF, Kimmel CB (1997) Musculoskeletal patterning in the pharyngeal segments of the zebrafish embryo. *Development* **124**, 2945–2960.

Schneider RA (1999) Neural crest can form cartilages normally derived from mesoderm during development of the avian head skeleton. *Dev Biol* **208**, 441–455.

Schuff M, Rossner A, Donow C, et al. (2006) Temporal and spatial expression patterns of *FoxN* genes in *Xenopus laevis* embryos. *Int J Dev Biol* **50**, 429–434.

Schuff M, Rossner A, Wacker SA, et al. (2007) FoxN3 is required for craniofacial and eye development of *Xenopus laevis*. *Dev Dyn* **236**, 226–239.

Schuff M, Siegel D, Bardine N, et al. (2010) *FoxO* genes are dispensable during gastrulation but required for late embryogenesis in *Xenopus laevis*. *Dev Biol* **337**, 259–273.

Scott KL, Plon SE (2003) Loss of Sin3∕Rpd3 histone deacetylase restores the DNA damage response in checkpoint-deficient strains of *Saccharomyces cerevisiae*. *Mol Cell Biol* **23**, 4522–4531.

Sedra SN, Michael MI (1957) The development of the skull, visceral arches, larynx and visceral muscles of the South African clawed toad, *Xenopus laevis* (Daudin) during the process of metamorphosis (from Stage 55 to Stage 66). Verh K Ned Akad Wet **51**, 1–80.

Seufert DW, Hall BK (1990) Tissue interactions involving cranial neural crest in cartilage formation in *Xenopus laevis* (Daudin). *Cell Differ Dev* **32**, 153–166.

Shigetani Y, Sugahara F, Kawakami Y, et al. (2002) Heterotopic shift of epithelial–mesenchymal interactions in vertebrate jaw evolution. *Science* **296**, 1316–1319.

Sokol OM (1977) Free swimming pipa larvae, with a review of pipid larvae and pipid phylogeny (Anura: Pipidae). *J Morphol* **154**, 357–425.

Stone LS (1926) Further experiments on the extirpation and transplantation of mesectoderm in *Amblystoma punctatum*. *J Exp Zool* **44**, 95–131.

Svensson ME, Haas A (2005) Evolutionary innovation in the vertebrate jaw: a derived morphology in anuran tadpoles and its possible developmental origin. *Bioessays* **27**, 526–532.

Taylor W, Van Dyke G (1985) Revised procedures for staining and clearing small fishes and other vertebrates for bone and cartilage study. *Cybium* **9**, 107–119.

Tokita M, Schneider RA (2009) Developmental origins of species-specific muscle pattern. *Dev Biol* **331**, 311–325.

Trainor PA, Tam PPL (1995) Cranial paraxial mesoderm and neural crest cells of the mouse embryo – codistribution in the craniofacial mesenchyme but distinct segregation in branchial arches. *Development* **121**, 2569–2582.

Tribioli C, Lufkin T (1997) Molecular cloning, chromosomal mapping and developmental expression of BAPX1, a novel human homeobox-containing gene homologous to *Drosophila* bagpipe. *Gene* **203**, 225–233.

Tribioli C, Frasch M, Lufkin T (1997) Bapx1: an evolutionary conserved homologue of the *Drosophila* bagpipe homeobox gene is expressed in splanchnic mesoderm and the embryonic skeleton. *Mech Dev* **65**, 145–162.

Trueb L, Hanken J (1992) Skeletal development in *Xenopus laevis* (Anura, Pipidae). *J Morphol* **214**, 1–41.

Umansky R (1966) The effect of cell population density on the developmental state of reaggregated mouse limb mesenchyme. *Dev Biol* **13**, 31–56.

Weisz PB (1945) The development and morphology of the larva of the South African clawed toad, *Xenopus laevis* 2. The hatching and the 1st-form and 2nd-form tadpoles. *J Morphol* **77**, 193–217.

Wilson J, Tucker AS (2004) Fgf and Bmp signals repress the expression of Bapx1 in the mandibular mesenchyme and control the position of the developing jaw joint. *Dev Biol* **266**, 138–150.

Ziermann JM, Olsson L (2007) Patterns of spatial and temporal cranial muscle development in the African clawed frog, *Xenopus laevis* (Anura: Pipidae). *J Morphol* **268**, 791–804.

Supporting Information

Additional Supporting Information may be found in the online version of this article:

Video S1. AVI film of 3D reconstructions (surface rendering) of a micro-CT analysis of an unilateral FoxN3-MO injected *Xenopus laevis* larvae showing first the chondrocranium and later the chondrocranium with the cranial musculature.

As a service to our authors and readers, this journal provides supporting information supplied by the authors. Such materials are peer-reviewed and may be re-organised for online delivery, but are not copy-edited or typeset. Technical support issues arising from supporting information (other than missing files) should be addressed to the authors.